




Effect of structural variation on enzymatic activity in tetranuclear (Cu₄) clusters with defective cubane core

M. Shahnawaz Khan, Mohd Khalid, M. Shahwaz Ahmad, Samrah Kamal, M. Shahid & Musheer Ahmad

To cite this article: M. Shahnawaz Khan, Mohd Khalid, M. Shahwaz Ahmad, Samrah Kamal, M. Shahid & Musheer Ahmad (2021): Effect of structural variation on enzymatic activity in tetranuclear (Cu₄) clusters with defective cubane core, Journal of Biomolecular Structure and Dynamics, DOI: [10.1080/07391102.2021.1924263](https://doi.org/10.1080/07391102.2021.1924263)


To link to this article: <https://doi.org/10.1080/07391102.2021.1924263>

 View supplementary material [↗](#)

 Published online: 27 May 2021.

 Submit your article to this journal [↗](#)




 Article views: 73

 View related articles [↗](#)

 View Crossmark data [↗](#)



Effect of structural variation on enzymatic activity in tetranuclear (Cu₄) clusters with defective cubane core

M. Shahnawaz Khan^a , Mohd Khalid^a, M. Shahwaz Ahmad^a, Samrah Kamal^a, M. Shahid^a  and Musheer Ahmad^b 

^aFunctional Inorganic Materials Lab (FIML), Department of Chemistry, Aligarh Muslim University, Aligarh, India; ^bDepartment of Applied Chemistry (ZHCET), Aligarh Muslim University, Aligarh, India

Communicated by Ramaswamy H. Sarma

ABSTRACT

The stimulus to the modeling of enzyme functioning sites comes from their potential to give insight into the natural enzyme's mechanistic pathways, ascertain the role of that different metal ion in the active site and construct better catalysts motivated by nature. The presence of metal ion leads to the activation of molecular oxygen in the metalloenzymes. The metalloenzymes such as the catechol oxidase (CO) enzyme that oxidizes the catechol to corresponding quinones which eventually protect damage tissues from plant and pathogen. Thus, the design and characterization of catalysts used as selectively and efficiently oxidation reactions have grown to be unique challenges for modern inorganic chemists. In this work, two novel tetranuclear complexes (**1** and **2**) have been synthesized in excellent yield. The complexes were characterized using various spectroscopic techniques such as FTIR, UV-Visible and PXRD pattern. The structure of **1** and **2** was elucidated by SC-XRD (single crystal X-ray diffraction) analysis. The magnetic study reveals the presence of the antiferromagnetic nature of **1** and **2**. Both **1** and **2** shows a very good catecholase-like activity by oxidizing the catechol to analogous quinone in methanolic solution. Thus, a structure-activity relationship can further help us design other substituted tetranuclear complexes with enhanced catecholase like activity.

ARTICLE HISTORY

Received 14 October 2020
Accepted 24 April 2021

KEYWORDS

Tetranuclear complexes;
copper cluster; defective
cubane; magnetism;
catecholase-like activity

1. Introduction

The coordination chemistry of the multinuclear complexes is nowadays most touted attractions owing to their potential topological specialties biological importance and material applications. Metal cluster plays a prominent role in catalysis (Khan et al., 2019; 2020; Wegner et al., 2001), bioinorganic chemistry (Ashafaq et al., 2020; Holm et al., 1996; Iman et al., 2019; Mariyam et al., 2020), and molecular magnetism (Ahamad et al., 2020; Khan et al., 2019; 2020). Amongst polynuclear cages and clusters, tetranuclear complexes of copper with cubane cores drag special attention due to their specific magnetism and catalytic properties (Papadakis et al., 2013). The tetranuclear complex also embodies a prototype system for metalloenzymes (Koval et al., 2006). In the last several years, the magnetic property of Cu₄O₄-type of complex with phenoxo, alkoxo, and hydroxo bridges has been investigated by various research groups by theoretical and experimental approaches (Scheme 1) (Fujita et al., 2001; Gungor et al., 2014; Mergehenn & Haase, 1977). After the development of first-ever single molecular magnets [Mn₁₂O₁₂(O₂CR)₁₆(H₂O)₄] (R = Ph, Me), which were synthesized unexpectedly by the reaction between Mn(III) and permanganate (Efthymiou et al., 2011; Kitos et al., 2011; Sessoli, Gatteschi, et al., 1993;

Sessoli, Tsai, et al. 1993), this proposal has become very admirable as it declares very skilled in constructing the large metal ion assemblies.

Furthermore, the oxidation process plays an influential role in the relevant synthesis of organic compounds viz. pharmaceuticals, agrochemicals, and some extra superior chemicals (Fontecave & Pierre, 1998; Que & Tolman, 2008). In the present scenario, consistent demands from society necessitate the progression of sustainable and atmosphere benign processes in manufacturing synthesis through the conventional oxidants method replacement, which is lethal and producing environmental pollution. Nowadays, there is an accelerating need for the discriminatory oxidation of natural compounds utilizing the dioxygen as a primary oxidant for manufacturing appliances because of its profitable and environmental reward. Though, the organic oxidation reaction by molecular oxygen is callous because of the inertness of molecular oxygen, which is associated with the triplet ground state of molecular oxygen; and this high-energy block is the way of nature to shield the organic compounds which are characteristically in the singlet ground state from unfavorable oxidation (Khan et al., 2019). Life has produced an artistic way to examine oxidations beneath normal circumstances in which metalloenzymes do activation of

molecular oxygen (Banu et al., 2009; Punniyamurthy et al., 2005). In recent times, many efforts have been employed from a bioinorganic chemist to treat an artificial analog approach on enzyme active-site (Castro et al., 2015; Dasgupta et al., 2017). From direct enzymatic reactions, this kind of information and insight is not available. Furthermore, extremely skilled biomimetic models may afford efficient biomimetic catalysts for the dilemma of conventional lethal inorganic catalysts for the industrialized process. Here it should be noted that the great catalytic action of metalloenzymes is chiefly correlating with the essential responsibility of protein chains that support substrate recognition and stabilization of the intermediate through various non-covalent forces (Dasgupta et al., 2017). Hence, the evolution of artificial analogs exceeding the first coordination sphere could be the right way to promote efficient biomimetic catalysts. Considering all the above things in our mind in the present work, we have synthesized two novel tetranuclear complexes using copper(II) metal salt employing amino alcohol and carboxylate ligands. The tetranuclear complexes are synthesized with the same experimental condition but a different synthetic procedure. In both the complexes, we have provided the basic medium using the NaOH, a strong base. The role of NaOH is crucial in forming both the complexes as it provides the template for the formation of defective cubane like structure. **1** was synthesized at pH = 8 while the **2** was isolated at little higher pH of 10. The synthesized complexes were characterized using various spectroscopic techniques and with the help of single crystal X-ray technique the exact structure of **1** and **2** was proposed. The design defective cubane established better catecholase-like activity and can be employed for magnetic materials in future endeavors.

2. Experimental protocols

2.1. General materials and measurements

All the chemicals used in this work are commercially available and used without any further purification. The copper nitrate trihydrate, 2-pyridine methanol, sodium hydroxide, benzoic acid, and 2-methoxy benzoic acid are reagent grade of Sigma-Aldrich and used as received. The whole characterization experiments were conducted at room temperature and pressure. The GX automatic recording spectrometer Perkin-Elmer spectrum was employed to understand the FTIR spectrophotometer as KBr disks from 4000 to 400 cm⁻¹. "MiniflexII X-ray diffractometer" having Cu-K α radiation was used to determine the PXRD patterns of complexes. The Perkin-Elmer Lambda-45 UV-visible spectrophotometer was used to check the electronic transition in **1** and **2** between 800–200 nm ranges at room temperature. The cuvettes use in the experiment was 1 cm path length. For the magnetic study, the temperature variable has been performed on an MPMS-XL quantum design SQUID magnetometer. The magnetic study was taken under an applied field of 0.1 T in the temperature range of 2–300 K. Further, the pascal constants were used for diamagnetic corrections.

2.2. Single-crystal X-ray analysis

Single-crystal XRD analysis of **1** and **2** was done at 100 K employing a Bruker SMART APEX CCD diffractometer. The data were monitored using graphite monochromated Mo-K α radiation with the $\lambda = 0.71073 \text{ \AA}$. The data reduction with integration has been made using the software named SAINT. The Empirical absorption adjustment was made with SADABS, and the determination of space group was performed with XPREP. DIFX commands fixed bond length parameters. The structures solution was done employing SHELXL-97, and refinement was performed on F^2 with full matrix least squares with SHELXL-97 (Ibers and Hamilton, 1974; Sheldrick, 2002; Bourhis et al., 2015). Anisotropic displacement parameters were used for refining H atoms. Table 1 illustrates the crystal data and refinement parameters for **1** and **2**. The CCDC number for **1** and **2** are 2036610 and 2036611.

2.3. Catecholase-like activity

Tetranuclear copper complexes were further checked to their biomimetic activity, such as the catecholase-like activity. In a methanolic solution standard substrate such as 3,5-di-*tert*-butyl catechol (3,5-DTBC) has been used to monitor the process of 3,5-DTBC oxidation to 3,5-di-*tert*-butylquinone (3,5-DTBQ). For monitoring the oxidation of 3,5-DTBC to 3,5-DTBQ, a Perkin-Elmer λ -45 absorption spectrophotometer was used. At 401 nm, the appearance of 3,5-DTBQ was observed after particular time intervals. Furthermore, the kinetics of catecholase like activity was also performed. In an experimental setup at a constant concentration ($\sim 1.0 \times 10^{-5}$ M) of complexes, and varying the concentration of 3,5-DTBC was taken in cuvettes and monitored it on UV-Visible spectrophotometer with different time intervals (Scheme 2). The curve between slopes of the absorbance versus time plot determined the underlying rate for catalyst-substrate combination. Michaelis–Menten method was used to understand the kinetic analyses, and Lineweaver–Burk plots were used to obtain all the critical kinetic parameters (Khan et al., 2020).

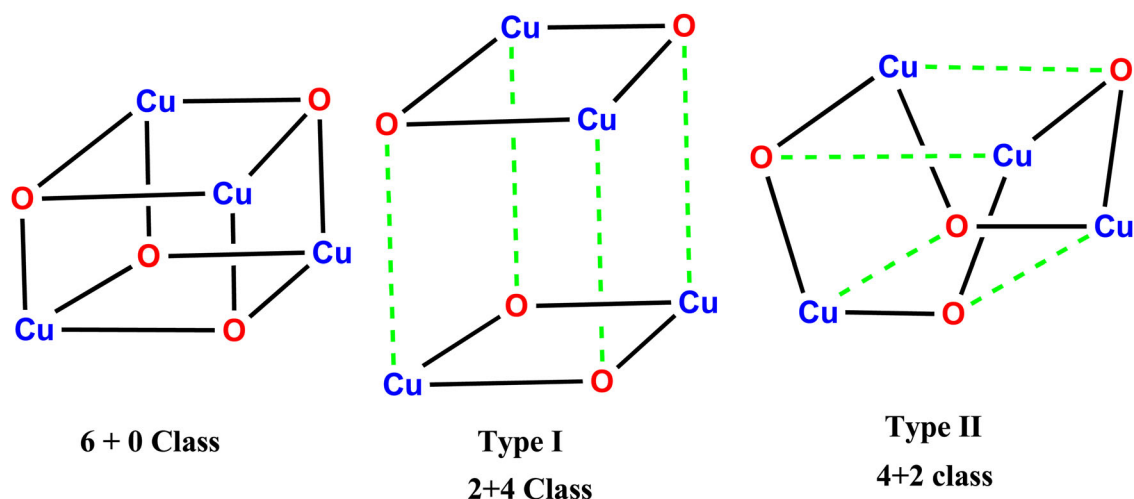
2.4. Synthetic protocols

The tetranuclear complexes **1** and **2** were synthesized using similar reaction conditions except for the pH of reactions. In case of **1**, the pH of the reaction was kept at 8 and in case of **2** the pH of the reaction was kept at 10 using aqueous NaOH (Scheme 3).

1 mmol of CuSO₄·5H₂O was poured in a round bottom flask with 15 mL of distilled water and 2-pyridine methanol (2 mmol). The whole reaction was stirred for almost an hour before adding the aqueous solution of 2 mmol benzoic acids (**1**) or 2-methoxy benzoic acid (**2**). The pH of the reaction was kept little basic to provide the template for the formation of tetranuclear complexes. Using the aqueous NaOH in **1** the reaction pH was kept at 8 and in **2** the pH of the reaction was kept at 10 and the whole mixture was stirred again for 3 h. After the reaction was completed, the solution was

Table 1. Crystallographic parameters for **1** and **2**.

Identification code	1	2
Empirical formula	C ₅₂ H ₄₆ Cu ₄ N ₄ O ₁₃	C ₄₈ H ₄₃ Cu ₄ N ₄ O ₁₃
Formula weight	1189.15	1138.08
Temperature/K	296(2)	100(2)
Crystal system	monoclinic	monoclinic
Space group	P2 ₁ /c	-P 2ybc
a/Å	20.819(5)	12.0799(8)
b/Å	13.021(4)	24.6243(16)
c/Å	19.561(5)	19.7876(14)
α/°	90	90
β/°	112.380(7)	103.959(2)
γ/°	90	90
Volume/Å ³	4904(2)	5712.2(7)
Z	4	4
ρ _{calc} /cm ³	1.6106	1.3233
μ/mm ⁻¹	1.782	1.527
F(000)	2430.5	2322.4252
Crystal size/mm ³	0.35 × 0.27 × 0.18	0.4 × 0.29 × 0.18
Radiation	Mo Kα (λ = 0.71073)	Mo Kα (λ = 0.71073)
Index ranges	-20 ≤ h ≤ 24, -15 ≤ k ≤ 12, -23 ≤ l ≤ 22	-16 ≤ h ≤ 16, -32 ≤ k ≤ 32, -26 ≤ l ≤ 26
Goodness-of-fit on F ²	1.050	1.0436
Final R indexes [I >= 2σ (I)]	R ₁ = 0.0703, wR ₂ = 0.1010	R ₁ = 0.1589 wR ₁ = 0.3178
Final R indexes [all data]	R ₁ = 0.1923, wR ₂ = 0.1352	R ₁ = 0.1474, wR ₂ = 0.3069

**Scheme 1.** Class of cubane as described in the literature.

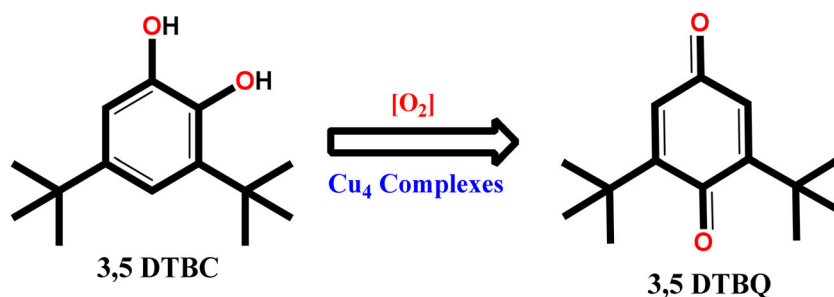
filtered off to remove the turbidity and kept in a beaker for slow evaporations. After several weeks blue color well-shaped crystals were obtained from the beakers.

3. Results and discussions

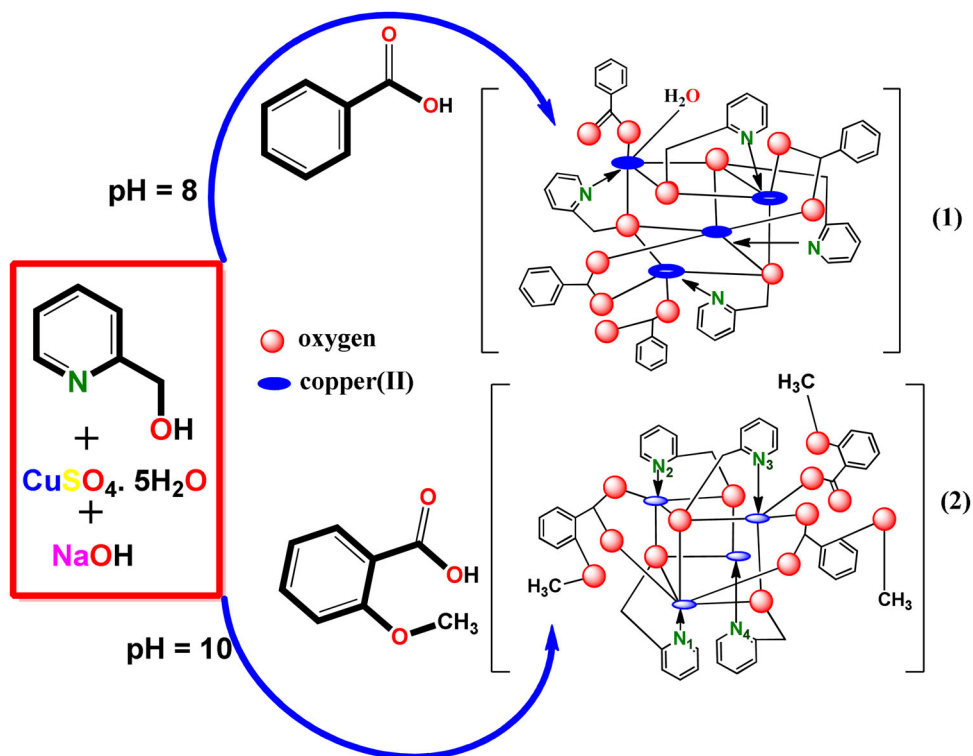
3.1. Synthetic approach

To understand the catalytic behavior of tetranuclear Cu(II) complexes we have design two defective cubane like structure in the presence of rigid amine 2-pyridine methanol (Hhmp) as primary ligand and benzoate ligand as a secondary ligand. In aqueous medium, sodium hydroxide (NaOH) has been used as pH regulator. Hhmp is a rigid amino

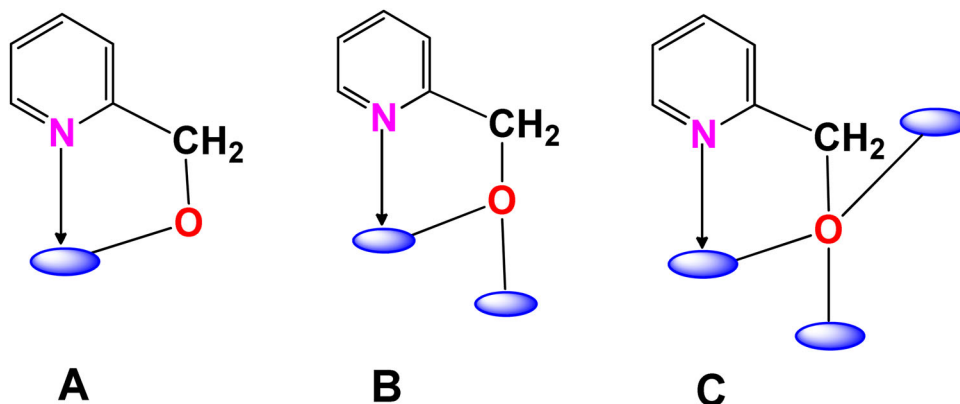
alcohol ligand with varying coordination chemistry. The ligand was previously used to synthesize numerous mono-, di- and polynuclear coordination complexes due to its unusual binding sites (Scheme 4). The synthetic procedure involves a simple method at ambient conditions to isolate two novel tetranuclear compounds containing Cu(II) metal ion. **1** was synthesized using the same environment at pH = 8 while **2** was isolated by changing the pH from 8 to 10 using aqueous NaOH. In the basic medium, the protonation of amino alcohol and benzoate ligand takes place very quickly. Moreover, the sturdy base, such as NaOH, provides the templates in the formation of tetranuclear copper complexes, which were further, explored for its unusual magnetic and catalytic properties. The distinctive structural features of **1** and **2** force us to



Scheme 2. Conversion of 3,5 DTBC into 3,5 DTBQ in presence of molecular oxygen.



Scheme 3. Synthetic route for 1 and 2.



Scheme 4. Different coordination modes of Hhmp ligand.

explore the chemistry associated with the defective cubane structure. **1** and **2** were thoroughly characterized, employing various spectroscopic and SC-XRD technique. With the assistance of single-crystal data, the molecular structure of **1** and **2** was established. The tetranuclear complexes are quite

robust, which is due to the presence of various non-covalent interactions in the compounds, especially C...H- π and π - π interactions. **1** and **2** were then employed to check if they can catalyze the organic reaction in the formation of 3,5-DTBQ from 3,5-DTBC in the presence of molecular oxygen.

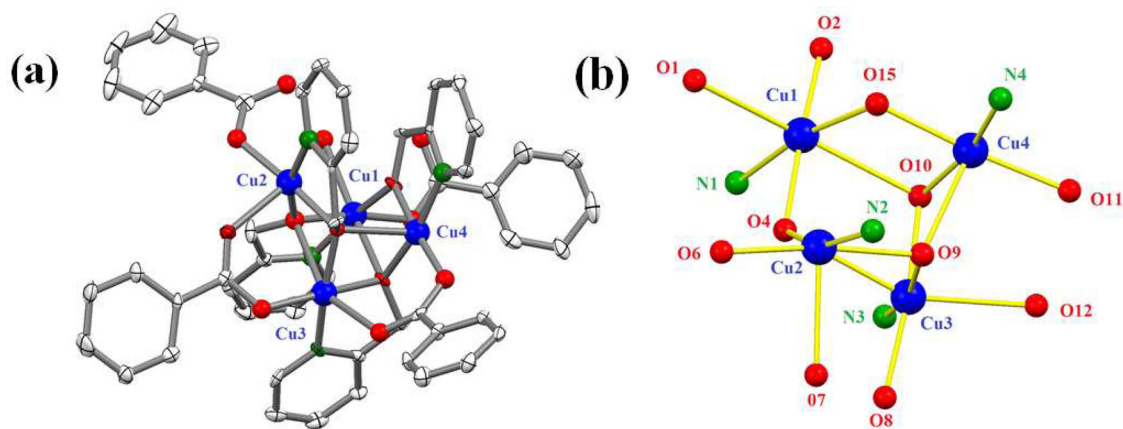


Figure 1. Molecular structure diagram of 1(a) and incomplete cubane core of 1 (b).

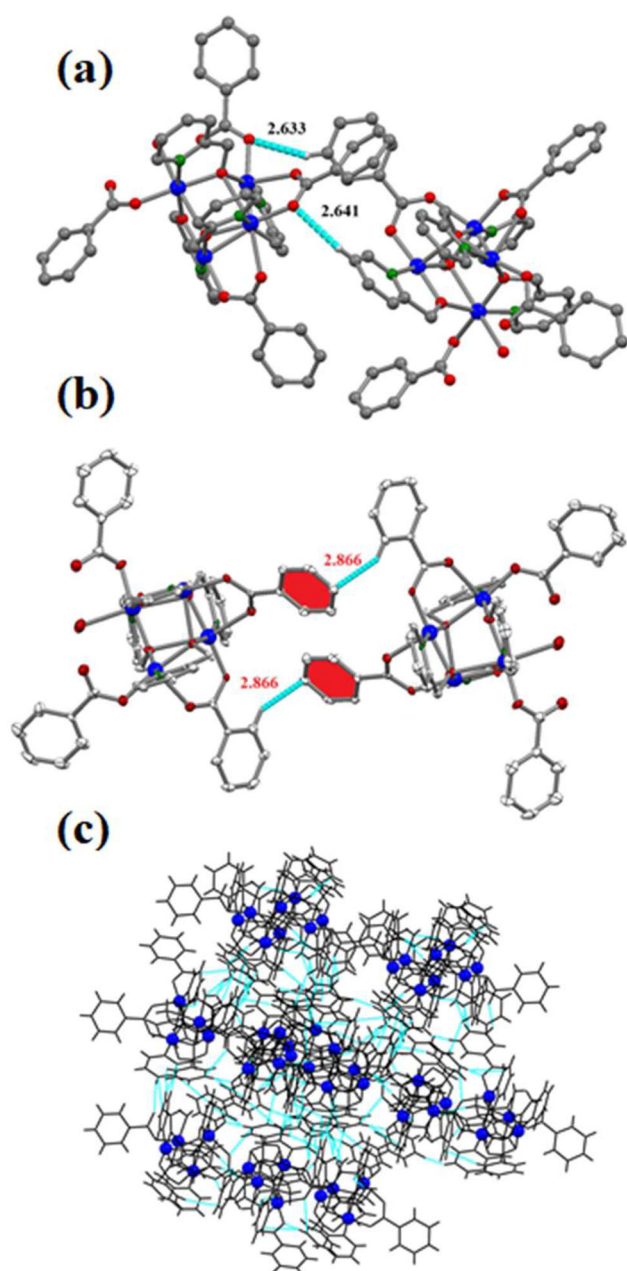
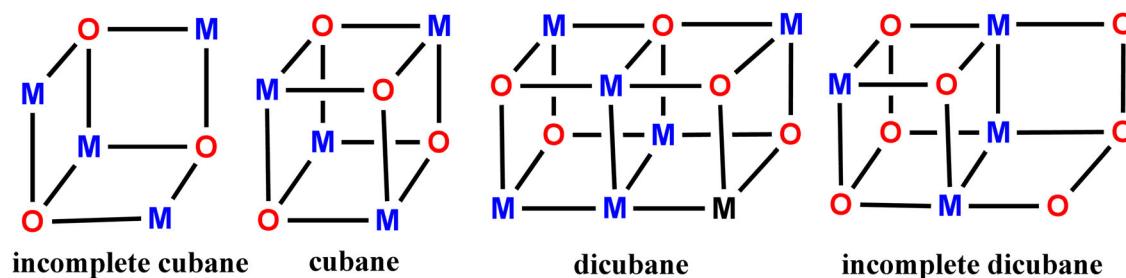


Figure 2. Formation of H-bonding (a), C-H- π bonding (b) and 3-D supra-molecular network (c) in 1.

3.2.1. Crystal description of $[\text{Cu}_4(\text{hmp})_4(\text{ba})_2(\text{Hba})_2(\text{H}_2\text{O})]$ (1)

The molecular structure of **1** is shown as Figure 1 (a), and the selected bond angles and bond distances are represented in Table S1 and S2 (supplementary material) ESI. The tetranuclear copper complexes were observed to be monoclinic having space group P21/c. The single-crystal X-ray data revealed that **1** is a tetranuclear copper (II) complex with the formula $[\text{Cu}_4(\text{hmp})_4(\text{ba})_2(\text{Hba})_2(\text{H}_2\text{O})]$ units and some solvent molecule also present in the lattice. The adjoining Cu_4 blocks disclose a single-open $[\text{Cu}_4(\mu_2\text{-O})(\mu_3\text{-O})_3]$ cubane core, as shown in Figure 1(b). The tetranuclear complex can be formed in various ways (Scheme 5). The tetranuclear copper(II) unit consists of four symmetrical Cu atoms with different coordination environments, two completely protonated chelating benzoic acid ligands (ba^{2-}), two partially protonated Hba $^-$ moiety and four hmp ligand. The five-coordinated Cu2 center is very similar to the five coordinated Cu4 metal ion. Cu4 atom confers a distorted square-pyramidal with $\{\text{Cu}_4\text{O}_4\text{N}\}$ environment with $\tau = 0.14$ and 0.214 for Cu2 and Cu4 metal ions. For an ideal square-pyramidal geometry, the Addison Tau parameter (τ) value is 0, and it is close to 1 for trigonal bipyramidal geometry. In both Cu2 and Cu4 center, the value of τ is close to 0, purporting the distorted square pyramidal geometry around the Cu2 and Cu4 metal ions (Bondi, 1964; Yang et al., 2007). Additionally, the four bond distances between the Cu2 or Cu4 and adjoining atom are nearly the same, but one bond is comparatively large, authenticating the square pyramidal geometry around Cu2 and Cu4 metal ions. The coordination environment around Cu2 ion filled by N2, O4, and O9 by amino alcohol ligand, O6 and O7 atom of benzoate ligand and N1, O4, and O10 by amino alcohol ligand, O1 and O2 by benzoate ligand. This equatorial N2, O4, O6, and O9 atom fills the position around Cu2 ion, $[\text{Cu2-N2 } 1.996(6) \text{ \AA}, \text{Cu2-O4 } 1.939(5) \text{ \AA}, \text{Cu2-O6 } 1.916(6) \text{ \AA}, \text{Cu}_2\text{-O9 } 1.974(5) \text{ \AA}]$ while the axial position is occupied by O7 atom $[\text{Cu2-O7 } 2.300(5) \text{ \AA}]$. Similarly, the equatorial position around Cu4 atom is occupied by N4, O9, O10 and O11 atom $[\text{Cu4-N4 } 1.980(6) \text{ \AA}, \text{Cu4-O9 } 2.312(5) \text{ \AA}, \text{Cu4-O10 } 1.924(4) \text{ \AA}, \text{Cu4-O11 } 1.941(5) \text{ \AA}]$. On the other hand, the Cu1 and Cu3 metal centers are present in distorted octahedral $\{\text{CuN}_2\text{O}_4\}$ atmosphere, filled by the N1 and N3 of amino alcohol ligand, O1, O2, O4, O15 and O4, O8, O9, O10



Scheme 5. Different type of cubane finds in the tetranuclear complexes.

of benzoate ligand. The axial position in Cu1 is invaded by N1, O1, O10 and O15 atom [Cu1-N1 1.995(6) Å, Cu1-O1 2.397(5) Å, Cu1-O10 2.449(5) Å, Cu1-O15 1.960(5) Å] and the equatorial places are occupied by O2 and O4 atom [Cu-O2 1.939(5) Å, Cu1-O4 1.939(5) Å]. The angle between O4-Cu1-O2, O10-Cu1-O1 and N3-Cu3-O9, O10-Cu3-O8 are 171.7(2), 165.97(17) and 166.8(2), 171.7(2) which deviates from a perfect linearity thus Cu1 and Cu3 metal centers ascertaining the coordination geometry as distorted octahedral. Some of the bond distances [i.e. Cu1-O1 2.397(5) Å, Cu3-O9 2.312(5) Å] are relatively long, but these are comparable to the sum of O and Cu atoms van der Waals radii (~2.92 Å) (Bondi, 1964; Yang et al., 2007). As displayed in Scheme 5, all the metal ions are interconnected jointly to each other via $[Cu_4(\mu_1-O)(\mu_3-O)_3]$ cubane core having Cu...Cu separation in the range of 2.9587(15) to 3.1007(15) Å (avg 3.329 Å). Several Ni_4 , Co_4 , Zn_4 , and Cu_4 complexes based on the 2-pyridine methanol have been documented in the literature (Lawrence et al., 2007; Yang et al., 2006; Zhang et al., 2013). These tetranuclear complexes having discrete cubane molecules displayed non-covalent interactions to form 1-D chains, but the discrete 0-D construction of **1** dispense a neutral tetra copper(II) $[Cu_4(hmp)_4(ba)_2(Hba)_2 \cdot H_2O]$ unit. Furthermore, the various non-covalent interactions (C-H... π , C-H...O, and π - π) can also be seen in the complex, contributing to forming a supramolecular network (Figure 2). One dimeric unit is connected to others through O-H...O hydrogen bonds; as a result, the 1-D polymeric chain is formed in compound **1** (Gronert & Keeffe, 2005; Mueller-Westerhoff et al., 1981).

3.2.2. Crystal description of $[Cu_4(hmp)_4(2Meba)_2(2MeHba)]$ solvent (2)

The discrete structure of **2** is present in a neutral tetranuclear form bearing the formula $[Cu_4(hmp)_4(2Meba)_2(2MeHba)]$ solvent, as depicted in Figure 3a. Although this tetranuclear complex somehow resembles **1**, there are some differences between the two structures. Complex **2** formed due to the contribution of four 2-pyridine methanol ligand, which binds to each copper ion into the protonated form, two 2-methoxy benzoic acid ligand in deprotonated form and one 2-methoxy benzoic acid ligand into its monoprotated form. There are also changes in the coordination environment around each copper metal atom. The Cu1 and Cu3 center is five coordinated systems with square pyramidal geometry, Cu2 is six coordinated distorted octahedron system, and Cu4 is four coordinated with square planer geometry. These few

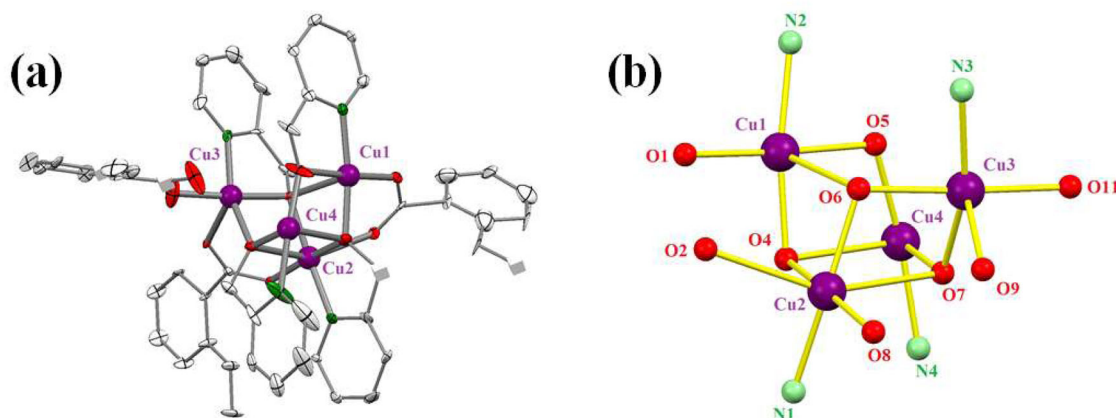
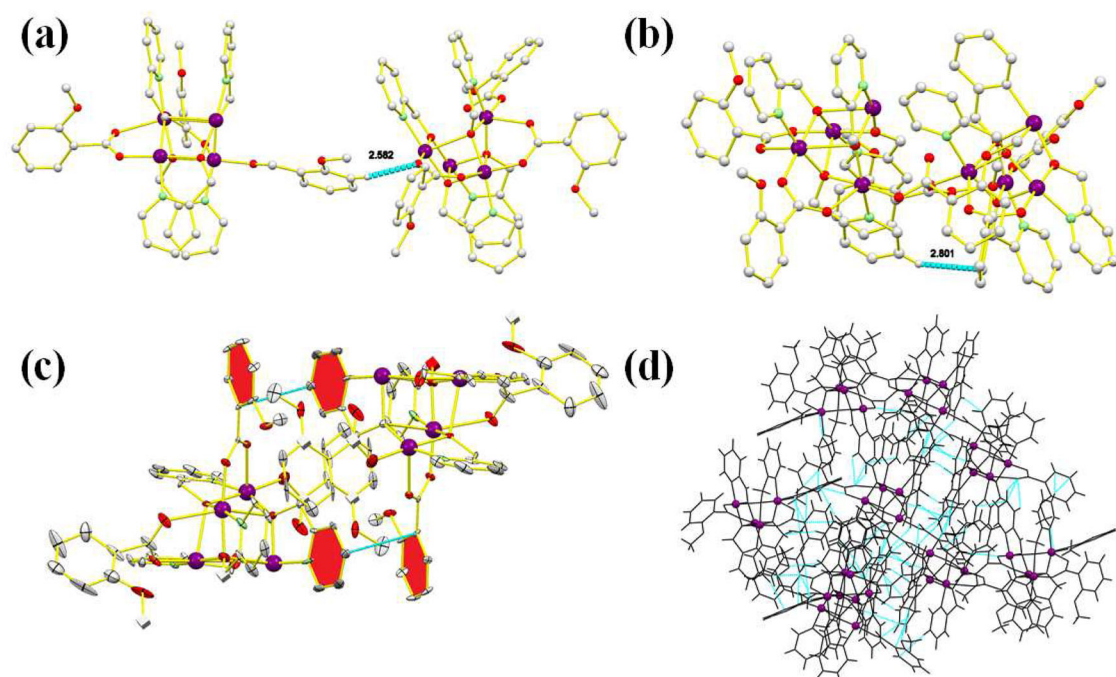
differences result in the formation of a slightly different open cubane core $[Cu_4(\mu_2-O)(\mu_3-O)_3]$ in **2**, as shown in Figure 3b. In **2**, resembling distorted square-pyramidal geometry was shown by Cu1 and Cu3 centers with $\{CuO_4N\}$ environments having $\tau=0.12$ and 0.22, respectively (Bondi, 1964; Yang et al., 2007). In the case of Cu1 center, the coordination sphere is filled by three O atoms of the three protonated amino alcohol ligands [Cu1-O4 1.925 Å; Cu1-O6 2.347 Å; Cu1-O5 1.943 Å], one O atom from the 3Meba moieties [Cu1-O1 1.944 Å] and one N atom of amino alcohol ligand [Cu1-N2 1.963 Å] bond distances. On the other hand, the five-coordination sphere around the Cu3 center is filled by two O atom of amino alcohol ligand, one N of amino alcohol ligand, and one atom of monoprotated deprotonated 3Meba ligands [Cu3-O6; Cu3-O9; Cu3-O11; Cu3-O7; Cu3-N3]. The coordination sphere around the Cu2 center is six coordinated distorted octahedral geometry filled with $\{CuO_5N\}$. The angle between N1-Cu2-O6, O4-Cu2-O8, and O2-Cu2-O7 deviates from linearity 180° to 169.67°, 173°, and 152° further confirming the distorted octahedral geometry around the Cu2 metal ion. The coordination sphere is filled by one N of amino alcohol ligand, three O atom of amino alcohol ligand, and two fully protonated O atom of 3Meba ligands [Cu2-N1 1.992(10) Å; Cu2-O7 1.920(8) Å; Cu2-O8=1.950(8) Å; Cu2-O4=1.960(10) Å; Cu2-O6=1.929(7) Å; Cu2-O2=2.445(10) Å]. The Cu4 center is present in square planer geometry around the central metal ion in $\{Cu_4NO_3\}$ with one N atoms of amino alcohol ligand and three O atom of amino alcohol ligand [Cu-N4 1.981(14) Å; Cu-O5 1.929(11) Å; Cu-O7 1.954(8) Å]. Several weak O-H, C-H... π and π - π interactions are also found in **2** (Figure 4) which contribute to crystal robustness; the C-H... π interactions are also created in the range of 2.801–2.810 Å between the one benzene ring of amino alcohol ligand and other rings of benzoate ligand. The π - π interaction specially provides the robustness of the structure formed between the two-benzene ring of amino alcohol ligand and a benzoate ligand results in a 1D polymer unit. H-bonding beside various non-covalent interactions is also being seen in the molecule, which contributes to the formation of a 3-D supramolecular network.

3.3. FTIR spectra of **1** and **2**

The Fourier Transform Infrared spectrum of designed tetranuclear complexes **1** and **2** have been recorded from 4000–400 cm^{-1} . Figure 5 shows the new band near 3410 cm^{-1} observed in **1** and 3390 cm^{-1} in **2** were due to

Table 2. Rate constants (s^{-1}) for the catechol oxidation reaction of previously reported tetranuclear Cu(II) complexes against substrate 3,5-DTBC.

S. No.	Complex	Solvent	k_{cat} (s^{-1})	Ref. No.
1.	$[Cu_4(L)(\mu OH)_2(H_2O)_4]5H_2O$	MeCN–water (pH = 7.5)	0.08	Mijangos et al. (2008)
2.	$[Cu_4(L_2)_4(MeOH)_2(ClO_4)_2]$	MeCN	0.045	Dasgupta et al. (2017)
3.	$[Cu_4(L_1)(\mu-O)(OAc)_4]$	MeCN; MeCN–water	0.0218	Dasgupta et al (2017)
4.	$[Cu_4(L_2)(OH)_4(Cl)_2](PF_6)_2$	CH ₂ Cl	0.0006	Sénèque et al. (2002)
5.	$[Cu_2(HL)(CO_3)(H_2O)]_2(CF_3SO_3)_4 \cdot 2CH_3CN \cdot 4H_2O$	MeOH	0.0002	Koval et al. (2006)
6.	$[Cu_4(O)(L)_2(Ac)_4]$	DMSO		Das et al. (2012)
7.	$[Cu_4(hmp)_4(ba)_2(Hba)_2]$	MeOH	0.36	This work
8.	$[Cu_4(hmp)_4(2Meba)_2(2MeHba)]$. solvent	MeOH	0.20	This work

**Figure 3.** Molecular labeling diagram of **2(a)**, and incomplete cubane core of **2(b)**.**Figure 4.** H-bonding (a), C-H- π bonding (b), robustness provided due to $\pi-\pi$ bonding (c) and formation 3-D network due to various non covalent interactions (d) in **2**.

$\nu(OH)$ in the complexes. Due to the amino alcohol ligand, the band is often seen in the three regions for **1** and **2**, i.e. 1) medium band in the 3400 cm^{-1} region is due to the alcoholic group. 2) The $\nu_{ass}(C-H)$ and $\nu_{sym}(C-H)$ vibration were also observed in the range of 2944 cm^{-1} and 2904 cm^{-1} ; 3) the three progressive bands around 1050 cm^{-1} assigned to

$\nu(C-O)$ (Gatehouse et al., 1958; Lever, 1984; Nakamoto, 1986). The vibration band in the region of $1610\text{--}1595\text{ cm}^{-1}$ is assigned to $\nu(C-C)$ due to the aromatic ring in **1** and **2**. The two consecutive bands at $1570/1384\text{ cm}^{-1}$ in **1** and $1506/1325\text{ cm}^{-1}$ in **2** are the characteristics band for $\nu_{ass}(COO^-)/\nu_{sym}(COO^-)$ of the carboxylate group attached to benzoate

ligand which has functional binding modes. It can bind to the central metal ion in bidentate or monodentate mode (Scheme S1 ESI), which depends upon the difference between $Z_v = \nu_{\text{asym}}(\text{COO}^-) - \nu_{\text{sym}}(\text{COO}^-)$. So, it can be said that **1** and **2** both are unsaturated carboxylates and can adopt bridging mono- or bidentate coordination modes with Z_v values observed at around 170 cm^{-1} . The magnitude of Z_v specifies that both **1** and **2** have an asymmetric bidentate mode and the anionic monodentate mode in **2**, which is also

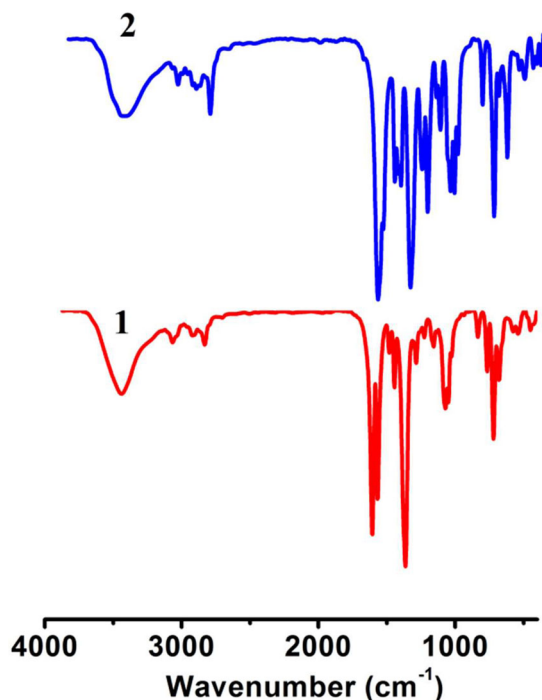


Figure 5. FTIR spectra of **1** and **2**.

authenticated by the SC-XRD of the complexes. There is no band in the range of 1385 cm^{-1} , justifying the absence of any anions present in **1** and **2**. The weak vibrational band of $\text{C}=\text{C}$ shifted at lower energy regions in case **1** and **2** (1620 cm^{-1}), symbolizing the significant influence of conjugation on the Hhmp aromatic ring. The aromatic ring hydrogens give rise to wagging vibration bands in $1459\text{--}1276\text{ cm}^{-1}$ and at 761 cm^{-1} (Khan et al., 2021; Krause et al., 1961). The $\text{C}-\text{C}$ bending vibrations of in-plane and out-of-plane are remarked at 650 and 416 cm^{-1} . The band at 950 cm^{-1} in **1** and **2** are characteristic of $\text{M}-\text{O}-\text{M}$ bridging. The bands that appeared at $590\text{--}800\text{ cm}^{-1}$ are related to deformation modes of the benzoate (ba) ligand. The weak intensity bands at $875\text{--}955\text{ cm}^{-1}$ are endorsed to the $\text{C}-\text{C}$ vibrations. The strong to medium bands in the region $953\text{--}1255\text{ cm}^{-1}$ may be due to the $\text{C}-\text{O}$ stretching vibrations of $\text{O}-\text{CH}_2$. The bands at $470\text{--}500\text{ cm}^{-1}$ (**1**) and $574\text{--}571\text{ cm}^{-1}$ (**2**) represents $\nu(\text{M}-\text{N})$ and $\nu(\text{M}-\text{O})$ vibrations, respectively (Frank & Rogers, 1966; Khan et al., 2021).

3.4. Electronic spectroscopic study

To understand the various transitions, involve in the tetranuclear complex, we have performed the electronic spectra of **1** and **2** (d^9) in 10^{-3} M concentration of methanol at ambient condition. The absorption spectra of the complexes exhibited well-resolved absorption bands at 212 , 261 , and 290 nm in **1** and 225 and 261 nm in **2** (Figure 6a). The two beautiful bands in **1** and **2** are assignable to intraligand ($n\rightarrow\pi^*$ and $\pi\rightarrow\pi^*$) charge transfer transitions. The broad absorption bands near 300 nm are characteristic of LMCT (ligand-to-metal charge transfer) in **1** and **2**. These peaks are consistent with the distorted octahedral geometry around

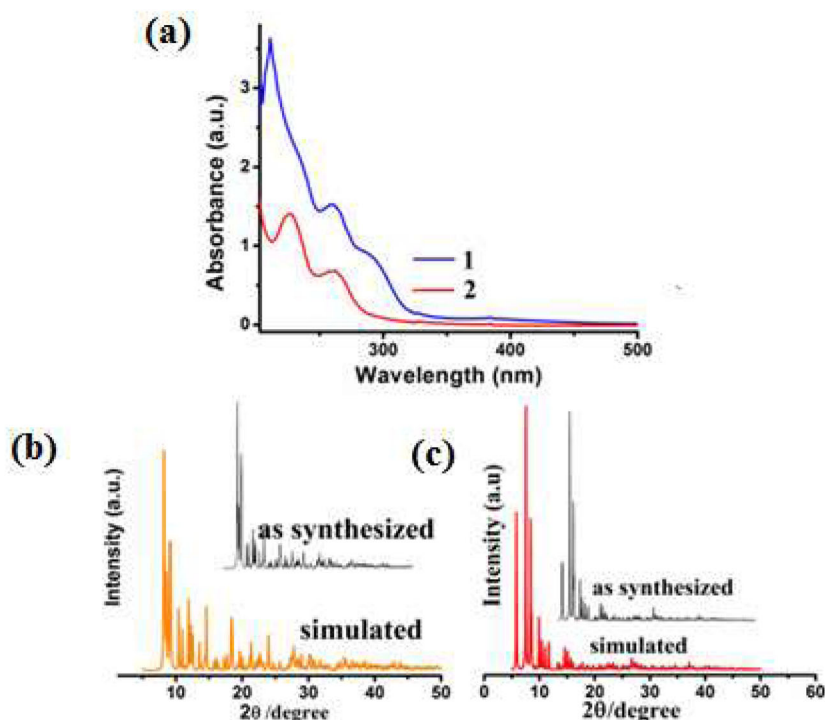


Figure 6. Electronic spectra (a) and PXRD pattern (b), (c) in **1** and **2**.

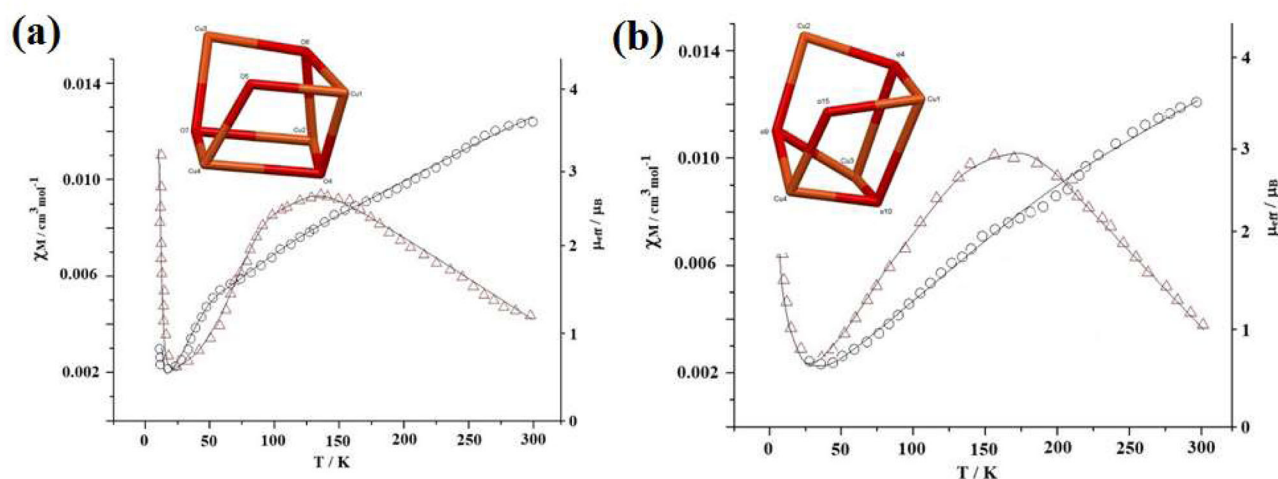


Figure 7. Plots of molar magnetic susceptibility ($\chi_M/\text{cm}^3\text{mol}^{-1}$) and effective magnetic moment (μ_{eff}/μ_B) versus temperature for **1**(a) and **2**(b). The experimental values are represented by hollow triangles and squares. The solid lines represent the best fit of the data.

the central metal ion. The slightly blue solution of **1** and **2** displayed low-intensity bands near 665 nm, which can be assigned to the d–d transition band (Amim et al., 2008; Ansari et al., 2016; Lever, 1984; Sama et al., 2017).

3.5. PXRD pattern of 1 and 2

The bulk purity of complexes was checked by performing powder XRD on as-synthesized crystals of both the complexes. These patterns were further compared with the simulated pattern, which was taken from the crystal data file. From Figure 6b and c, it is clear that the PXRD pattern of synthesized and simulated crystals is almost identical, authenticating the bulk purity of **1** and **2** (Kamal et al., 2020).

3.6. Magnetic study

The magnetic susceptibility measurements were performed for **1** and **2** in the temperature range of 2–300 K under a 0.1 T magnetic field. As shown in Figure 7, with when temperature is decreased, the susceptibility increases steadily to a maximum up to 144 K (**1**) or 156 K (**2**) and then decreases rapidly. On the other hands, the μ_{eff} decreases continuously upon cooling upto 43 K in **1** and 47 K in **2** and indicating an antiferromagnetic behavior. The susceptibility increases slightly at less than 30 K, probably due to the presence of a small amount of paramagnetic impurity (Merz & Haase, 1978; 1980). At room temperature, the $\chi_M T$ values for **1** and **2** are 1.27 and 1.21 $\text{cm}^3 \text{kmol}^{-1}$ which are slightly lesser than the expected value (1.50 $\text{cm}^3 \text{kmol}^{-1}$) for uncoupled four spin-only Cu^{2+} ions ($S = 1/2$). For the incomplete cubane structures of **1** and **2**, the isotropic exchange integral J_{ij} is used to describe the coupling interactions, by which the Heisenberg spin–spin exchange Hamiltonian equation (1) has been produced. Considering the paramagnetic impurities and temperature independent magnetic susceptibility $N\alpha$, the van Vleck equations (2) and (3) of the appropriate molar magnetic susceptibility can be applied to fit the experiment plot. The fitting parameters provide, $J = -47.33 \text{ cm}^{-1}$, $J' = -2.97 \text{ cm}^{-1}$, $g = 2.06$, $x = 0.015$

($R = 4.12 \times 10^{-4}$) for **1** and $J = -44.61 \text{ cm}^{-1}$, $J' = -3.11 \text{ cm}^{-1}$, $g = 2.06$, and $x = 0.013$ ($R = 4.12 \times 10^{-4}$) for **2**, where $x = a$ small paramagnetic impurity.

$$H = -2J(S_1S_2 + S_3S_4) - 2J'(S_1S_3 + S_1S_4 + S_2S_3 + S_2S_4) \quad (1)$$

$$\chi_{\text{tet}} = [\text{Nb}^2 g^2 / 4kT] (10e^{2u} + 2e^{-2u} + 4e^{-2v}) / (5e^{2u} + 3e^{-2u} + e^{-4u} + 6e^{-2v} + e^{-4v}) \quad (2)$$

where $u = J/kT$ and $v = J'/kT$

$$\chi_M = (1 - x)\chi_{\text{tet}} + [x \cdot N\beta^2 g^2 / 4kT] + N\alpha \quad (3)$$

$$R = \frac{\sum (\chi_M^{\text{calc}} T - \chi_M^{\text{exp}} T)^2}{\sum (\chi_M^{\text{exp}} T)^2}$$

The data reveal the presence of both strongly antiferromagnetic (between bridged Cu(II) centers) and weakly anti-ferromagnetic interactions (between weakly bridged Cu(II) centers). The present results are quite different from the reported similar cubane complexes (Tan et al., 1999; Walz et al., 1983) which exhibit both ferromagnetic and antiferromagnetic interactions. The difference in the J values in the two cubane (**1** and **2**) could be due to the presence of the inductive effect group and the slight variations in the bond angles which bridge the two neighboring Cu(II) centers. The geometry, i.e., distorted octahedral may also be the reason of the presence of only antiferromagnetic interactions rather than both antiferro and ferro- magnetic (as reported in literature in such cubane cores) (Tan et al., 1999; Walz et al., 1983).

3.7. Catecholase like activity

Catechol oxidase is a dinuclear copper complex, and in the appearance of molecular oxygen, it catalyzes the oxidation of catecholase to the analogous quinone. In the latter several years, a considerable number of mononuclear, dinuclear, and polynuclear copper and other transition metal complexes are designed for the model of catecholase oxidase (Liu et al., 2015). The preferential oxidation of catechol to its corresponding quinone is of exceptional significance for the hormonally vigorous catecholamines (Ahmad et al., 2020;

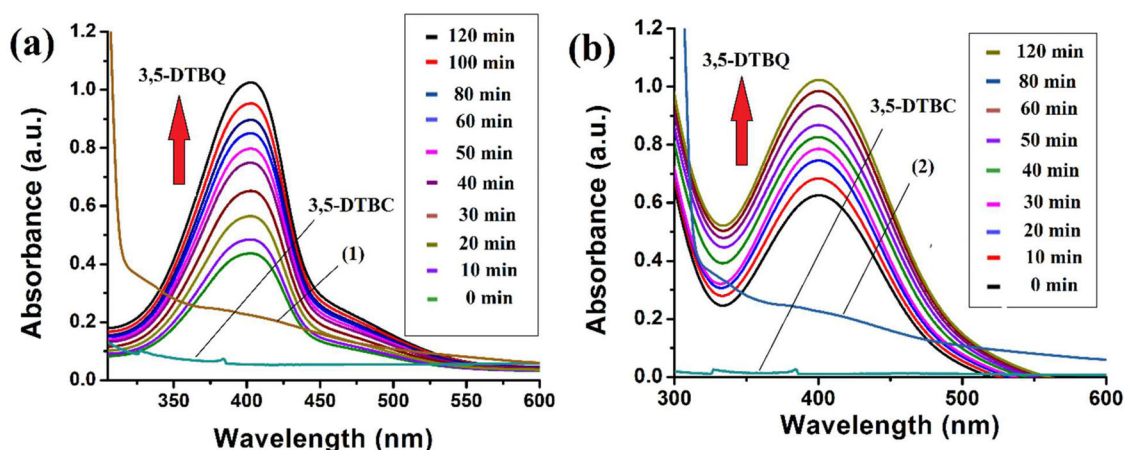


Figure 8. Formation of 3,5-DTBQ with increasing time in 1(a) and 2(b).

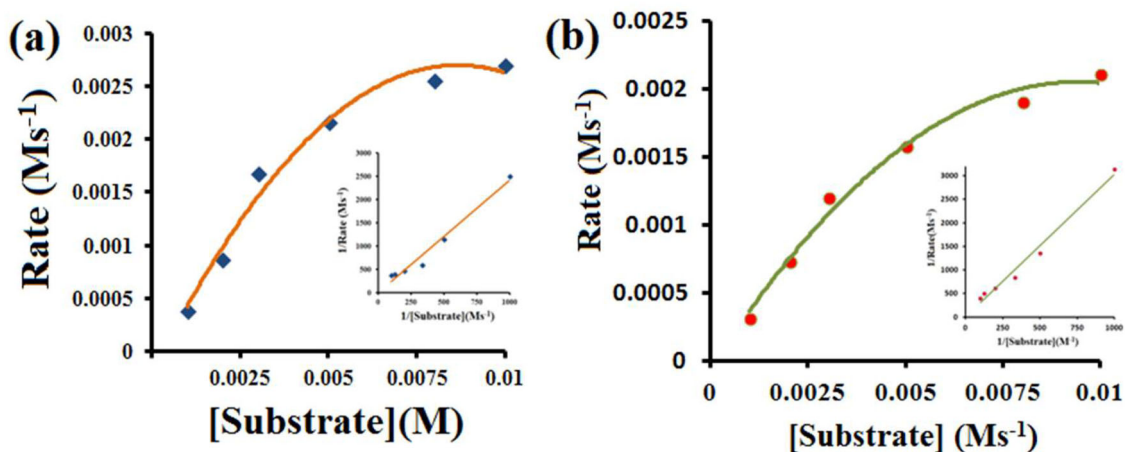


Figure 9. Kinetics of 1(a) and 2(b).

Ahmad et al., 2020; Sama et al., 2017). In this work, we have studied the oxidation of 3,5-DTBC to 3,5-DTBQ in the methanolic solution. The selective oxidation of 3,5-DTBC is fundamental to monitor and is frequently used as a diagnostic reaction for new biomimetic copper complexes. The UV-Vis scan used for observing the conversion of 3,5-DTBC to 3,5-DTBQ by seeing the absorbance at 401 nm for the construction of 3,5-DTBQ as a function of time. In a laboratory setup, 10^{-4} M solutions of **1** or **2** were added in 10^{-2} M solution of the 3,5-DTBC into a 1:1 ratio. At 25 °C and the experiment was performed in a methanol solvent. The reaction was followed for 2 h after the addition of 3,5-DTBC into the solution of **1** and **2**. Both **1** and **2** were active to serve as a mimic for catechol oxidase. Initially, **1**, and **2** does not dispense band in the range of 401 nm, but after 3,5-DTBC, it shows a developing peak as manifested in Figure 8. The formation of quinone at 401 nm provides the distinct sign for 3,5-DTBQ and signifies that **1** and **2** are catalytically active. The other catalytic performance of the complexes may be due to the unusual coordination environments around **1** and **2** in an open cubane structure. The results indicate that in both cases, the oxidation of 3,5-DTBC to the analogous 3,5-DTBQ was highly dependent on the time of reaction. In the presence of molecular oxygen, **1** and **2** shows excellent catalytic activity, but when the same reaction was performed in the

presence of copper nitrate, no conversion was observed after 120 min. This indicates that **1** and **2** can act as a catalyst in the translation of 3,5-DTBC to 3,5-DTBQ, proving the efficiency of **1** and **2**. The way copper metal linking to the benzoate and amino alcohol ligand helped to sustain the solid structure favoring the catalytic routine, although the degree to which this configuration is imperative for catalysis is unidentified. One thing should be noted that the way Cu(II) differently bind to the ligands can also have some role in the catecholase like activity of **1** and **2**. The different catalytic activity for earlier documented model complexes is frequently ascribed to the redox potentials, intermetallic Cu–Cu distance, coordination spheres, and neighboring groups. A large number of mono-, di- and polynuclear complexes of Cu(II) ion as functional mimics for catechol oxidase have been well documented in the literature (Adak et al., 2016; Ahmad et al., 2020; Ording-Wenker et al., 2015), but with this combination of ligands, this is a very first example of catecholase like activity was explored.

3.8. Kinetics study of complexes

Understanding the mechanism inside the catalytic reaction, kinetic experiments were carried out on the tetranuclear complexes (taking a constant concentration of 10^{-4} mol

dm⁻³) and varying the concentration from 10⁻³ to 10⁻² mol dm⁻³ of 3,5-DTBC. The whole experiment was monitored by UV-vis spectrophotometry. First, the stock solutions of **1**, **2**, and substrate were prepared in methanol. The UV-vis quartz cell was filled with 2 ml of a substrate having an exact concentration formed by diluting the stock solution. The quartz cell was left for a while inside the cell holder attached with a thermostat maintaining the 25 °C temperature. A known amount of stock solution of **1** or **2** added to it to attain a preferred concentration of **1** and **2** as 10⁻⁴ mol dm⁻³ with increasing time formation of 3,5-DTBQ was monitored. The classical rate method was employed to verify the rate constant for each substrate concentrations, and each experiment was repeated three times. For both the complexes, the value of the average rate constant point toward the rate is first order at low concentrations of the substrate. It is clear from Figure 9 dependencies on the initial rate on the concentration of the substrate. This type of saturation reaction depends on catechol concentration and can be effortlessly inherent by applying the Michaelis–Menten equation for kinetics. The above mechanism leads to the well-known Michaelis–Menten equations: (Banu et al., 2009)

$$V = \frac{V_{\max}[S]}{K_m + [S]} \quad (4)$$

$$K_M = (k_2 + k_3)/k_1 \quad (5)$$

where V denotes initial rate, $[S]$ denotes the substrate concentration, K_m is Michaelis–Menten constant for the tetranuclear complex, and V_{\max} = maximum initial rate for a specific concentration the complexes in the incidence of 3,5-DTBC. To plot the data, the Michaelis–Menten equation can be modified into other easy forms. The most widely used transform equation known as Lineweaver–Burk equation as follows:

$$\frac{1}{V} = \frac{K_m}{V_{\max}} \cdot \frac{1}{[S]} + \frac{1}{V_{\max}} \quad (6)$$

From the above equation, the value of K_M and V_{\max} can be calculated, and the value of k_{cat} was calculated by dividing the V_{\max} values with complex concentration. After the calculation for complex **1** the values of $k_{\text{cat}} = 1297.6 \text{ h}^{-1}$, $V_{\max} = 0.3604 (10^{-4} \text{ M s}^{-1})$, and $K_m = 0.8702 (10^{-4} \text{ M})$ and for complex **2** the values are $K_{\text{cat}} = 748.58 \text{ h}^{-1}$, $V_{\max} = 0.2078 (10^{-4} \text{ M s}^{-1})$, and $K_m = 0.6292 (10^{-4} \text{ M})$, respectively. When the kinetic parameters of **1** and **2** were compared, it was found that **1** shows better K_{cat} value than that of **2**. This difference between the kinetic parameters is due to the different groups situated on the benzoate ligand. The methoxy group on the ortho position of benzoic acid has a great effect on the catalytic activity of **2**. Due to H atom's presence on the ortho position of **1**, it is obvious that one enhances the catalytic activity. The phenomenon can be easily justified by considering the different electron-donating substituents capabilities on the ortho positions of the auxiliary ligand. This hypothesis can be further verified by the work published by S. Gao et al., where the catalytic activity follows the $\text{CH}_3 > \text{H} > \text{OH} > \text{Cl}$ order. In this case, the complex containing the CH_3 group shows better catalytic activity due to higher

electron-donating capability (Sreenivasulu et al., 2006). We can take another example in which the research group of Torelli elaborates on the catalytic activity of some dinuclear copper complexes using H-BPMP-type ligands. In that research article, they saw the drastic modulation of activities by the substituent of para-positions. Using the methyl-substituted ligand as a reference, the activity was found to be inhibited to a moderate extent when substituted by a strong electron-withdrawing F atom, and the opposite was reported to be true for the electron-donating $-\text{OCH}_3$ group (Belle et al., 2002). Based on previous literature and our understanding of chemistry, we can draw a definite conclusion about the effect of substituent and their electronegativity on the catecholase like activity of **1** and **2**. To deeply understand the steric encumbrance on the α -carbon of the carboxylate group also affect the oxidation of 3,5-DTBC to 3,5-DTBQ. Likewise, Karlin and Casella suggested that the mechanism associated with the oxidation of catechol to the corresponding quinone by some dinuclear complexes, and they proposed that in the second step, two electrons of the catecholase reduce the copper(II) to copper(I) after transfer of two protons to the bridging alkoxide groups (Karlin et al., 1994; Karlin et al., 1993; Battaini et al., 2000). The kinetic parameters of these two newly designed tetranuclear complexes have been compared with those of some of the tetranuclear copper(II) complexes already reported in the literature (Table 2). The catecholase activity of the present complexes is moderate for oxidizing 3,5-DTBC into corresponding quinone (Das et al., 2012).

4. Conclusion

In summary, two discrete assemblies of copper atoms have been lucratively designed employing a polyalcohol and carboxylate ligand *via* the slow evaporation method. **1** and **2** are constructed in the basic medium using strong base NaOH as a pH regulator in the reaction. **1** and **2** were characterized by different spectral techniques. Tetranuclear copper complexes have scaffold Cu_4O_4 cubane [4+2]-type structure, verified by single-crystal XRD analysis. The molecular formula of **1** and **2** were formulated as $[\text{Cu}_4(\text{hmp})_4(\text{ba})_2(\text{Hba})_2\text{H}_2\text{O}]$ and $[\text{Cu}_4(\text{hmp})_4(2\text{Meba})_2(2\text{MeHba})]$ solvent. The open cubane like structures of **1** and **2** having unusual catalytic and magnetic properties. Magnetic data elaborate on the moderate antiferromagnetic nature of the tetranuclear complexes. The tetranuclear complexes have the same structural features and can act like those of naturally occurring catecholase enzymes. The catecholase like activity of both **1** and **2** was elaborated, and their kinetic parameters were also calculated.

Acknowledgments

The author thanks chairperson, Department of Chemistry, AMU, Aligarh, for providing the necessary research facilities. M. S. Khan thanks UGC, New Delhi, for providing a Non-NET Fellowship. M. Khalid gratefully acknowledges UGC, New Delhi, for providing start up grant. Author also thank to UGC DRS-SAP (II) and DST-FIST program for financial assistance.

Disclosure statement

No potential conflict of interest was reported by the author(s).

ORCID

M. Shahnawaz Khan  <http://orcid.org/0000-0002-3631-1914>

M. Shahid  <http://orcid.org/0000-0003-3817-0286>

Musheer Ahmad  <http://orcid.org/0000-0002-7446-0232>

References

- Adak, P., Ghosh, B., Bauzá, A., Frontera, A., Blake, A. J., Corbella, M., Das Mukhopadhyay, C., & Chattopadhyay, S. K. (2016). Catecholase activity, DNA binding and cytotoxicity studies of a Cu(II) complex of a pyridoxal schiff base: Synthesis, X-ray crystal structure, spectroscopic, electrochemical and theoretical studies. *RSC Advances*, 6(90), 86851–86861. <https://doi.org/10.1039/C6RA14059A>
- Ahamad, M. N., Iman, K., Raza, M. K., Kumar, M., Ansari, A., Ahmad, M., & Shahid, M. (2020). Anticancer properties, apoptosis and catecholase mimic activities of dinuclear cobalt(II) and copper(II) Schiff base complexes. *Bioorganic Chemistry*, 95, 103561. <https://doi.org/10.1016/j.bioorg.2019.103561>
- Ahamad, M. N., Khan, M. S., Shahid, M., & Ahmad, M. (2020). Metal organic frameworks decorated with free carboxylic acid groups: Topology, metal capture and dye adsorption properties. *Dalton Transactions (Cambridge, England: 2003)*, 49(41), 14690–14705. <https://doi.org/10.1039/d0dt02949a>
- Ahmad, M. S., Khalid, M., Khan, M. S., Shahid, M., & Ahmad, M. (2020). Synthesis, characterization, and catecholase mimic activity of a new 1D Cu(II) polymer constructed from iminodiacetate. *Journal of Structural Chemistry*, 61(4), 533–540. <https://doi.org/10.1134/S0022476620040058>
- Ahmad, M. S., Khalid, M., Khan, M. S., Shahid, M., Ahmad, M., Rao, M., Ansari, A., & Ashafaq, M. (2020). Exploring catecholase activity in dinuclear Mn(II) and Cu(II) complexes: an experimental and theoretical approach. *New Journal of Chemistry*, 44, 7998–8009.
- Amim, R. S., Oliveira, M. R. L., Perpetuo, G. J., Janczak, J., Miranda, L. D. L., & Rubinger, M. M. M. (2008). Syntheses, crystal structure and spectroscopic characterization of new platinum(II) dithiocarbamate complexes. *Polyhedron*, 27(7), 1891–1897. <https://doi.org/10.1016/j.poly.2008.02.030>
- Ansari, I. A., Sama, F., Shahid, M., Rahisuddin, R., Arif, R., Khalid, M., & Siddiqi, Z. A. (2016). Isolation of proton transfer complexes containing 4-picolinium as cation and pyridine-2,6-dicarboxylate complex as anion: Crystallographic and spectral investigations, antioxidant activities and molecular docking studies. *RSC Advances*, 6(14), 11088–11098. <https://doi.org/10.1039/C5RA25939H>
- Ashafaq, M., Khalid, M., Raizada, M., Ahmad, M. S., Khan, M. S., Shahid, M., & Ahmad, M. (2020). A Zn-based fluorescent coordination polymer as bifunctional sensor: sensitive and selective aqueous-phase detection of picric acid and heavy metal ion. *Journal of Inorganic and Organometallic Polymers and Materials*, 30(11), 4496–4509. <https://doi.org/10.1007/s10904-020-01579-6>
- Banu, K. S., Chattopadhyay, T., Banerjee, A., Mukherjee, M., Bhattacharya, S., Patra, G. K., Zangrando, E., & Das, D. (2009). Mono- and dinuclear manganese(III) complexes showing efficient catechol oxidase activity: Syntheses, characterization and spectroscopic studies. *Dalton Transactions*, (40), 8755–8764. <https://doi.org/10.1039/b902498k>
- Battaini, G., Monzani, E., Casella, L., Santagostini, L., & Pagliarini, R. (2000). Inhibition of the catecholase activity of biomimetic dinuclear copper complexes by kojic acid. *Journal of Biological Inorganic Chemistry: A Publication of the Society of Biological Inorganic Chemistry*, 5(2), 262–268. <https://doi.org/10.1007/s007750050370>
- Belle, C., Beguin, C., Gautier-Luneau, I., Hamman, S., Philouze, C., Pierre, J. L., Thomas, F., & Torelli, S., Saint-Aman, E., & Bonin, M. (2002). Dicopper(II) complexes of H-BPMP-TYPE LIGANDS: pH-induced changes of redox, spectroscopic (¹⁹F NMR studies of fluorinated complexes), structural properties, and catecholase activities. *Inorganic Chemistry*, 41, 479–491.
- Bondi, A. (1964). van der Waals Volumes and Radii. *The Journal of Physical Chemistry*, 68(3), 441–451. <https://doi.org/10.1021/j100785a001>
- Bourhis, L. J., Dolomanov, O. V., Gildea, R. J., Howard, J. A. K., & Puschmann, H. (2015). Crystal structure of 5,11-diethyl-2,3,4,5-tetrahydro-1,4-benzodiazepin-6-one. *Acta Crystallographica, Section A*, 71, 59–60.
- Castro, K. A. D. F., Simões, M. M. Q., Neves, M. G. P. M. S., Cavaleiro, J. A. S., Ribeiro, R. R., Wypych, F., & Nakagaki, S. (2015). Synthesis of new metalloporphyrin derivatives from [5,10,15,20-tetrakis(pentafluorophenyl)porphyrin] and 4-mercaptobenzoic acid for homogeneous and heterogeneous catalysis. *Applied Catalysis A: General*, 503, 9–19. <https://doi.org/10.1016/j.apcata.2014.12.048>
- Das, D., Guha, A., Das, S., Chakraborty, P., Mondal, T. K., Goswami, S., & Zangrando, E. (2012). Diastereomerism in tetranuclear copper(II) complexes of a phenol based “end-off” compartmental ligand. *Inorganic Chemistry Communications*, 23, 113–116. <https://doi.org/10.1016/j.inoche.2012.06.020>
- Dasgupta, S., Majumder, I., Chakraborty, P., Zangrando, E., Bauza, A., Frontera, A., & Das, D. (2017). Ligand-flexibility controlled and solvent-induced nuclearity conversion in Cu(II)-based catecholase models: A deep insight through combined experimental and theoretical investigations. *European Journal of Inorganic Chemistry*, 2017(1), 133–145. <https://doi.org/10.1002/ejic.201600985>
- Efthymiou, C. G., Papatrifaftyllopoulou, C., Aromi, G., Teat, S. J., Christou, G., & Perlepes, S. P. (2011). A Ni(II) cubane with a ligand derived from a unique metal ion-promoted, crossed-aldol reaction of acetone with di-2-pyridyl ketone. *Polyhedron*, 30(18), 3022–3025. <https://doi.org/10.1016/j.poly.2011.02.024>
- Fontecave, M., & Pierre, J.-L. (1998). Oxidations by copper metalloenzymes and some biomimetic approaches. *Coordination Chemistry Reviews*, 170, 125–140.
- Frank, C. W., & Rogers, L. B. (1966). Infrared spectral study of metal-pyridine, -substituted pyridine, and -quinoline complexes in the 667–150 cm⁻¹ region. *Inorganic Chemistry*, 5(4), 615–622. <https://doi.org/10.1021/ic50038a026>
- Fujita, M., Umemoto, K., Yoshizawa, M., Fujita, N., Kusukawa, T., & Biradha, K. (2001). Molecular paneling via coordination. *Chemical Communications* (6), 509–518. <https://doi.org/10.1039/b008684n>
- Gatehouse, M., Livingstone, S. E., Nyholm, R. S., & Inorg, J. (1958). Infrared spectra of some nitrate and other oxy-anion co-ordination complexes. *Journal of Inorganic and Nuclear Chemistry*, 8, 75–78. [https://doi.org/10.1016/0022-1902\(58\)80166-9](https://doi.org/10.1016/0022-1902(58)80166-9)
- Gronert, S., & Keeffe, J. R. (2005). Identity hydride-ion transfer from c-h donors to c-acceptor sites. enthalpies of hydride addition and enthalpies of activation. Comparison with C-H...C proton transfer. An ab initio study. *Journal of the American Chemical Society*, 127(7), 2324–2333. <https://doi.org/10.1021/ja044002l>
- Gungor, E., Kara, H., Colacio, E., & Mota, A. J. (2014). Two tetranuclear Copper(II) complexes with open cubane-like Cu₄O₄ core framework and ferromagnetic exchange interactions between Copper(II) ions: structure, magnetic properties, and density functional study. *European Journal of Inorganic Chemistry*, 2014(9), 1552–1560. <https://doi.org/10.1002/ejic.201301515>
- Holm, R. H., Kennepohl, P., & Solomon, E. I. (1996). Structural and functional aspects of metal sites in biology. *Chemical Reviews*, 96(7), 2239–2314. <https://doi.org/10.1021/cr9500390>
- Ibers, J. A., & Hamilton, W. C. (1974). *International tables for X-ray crystallography* [IV 26 SMART & SAINT Software Reference manuals, Version 6.45], 2003. Kynoch Press/Bruker Analytical X-ray Systems, Inc., 2003.
- Iman, K., Shahid, M., Khan, M. S., Ahmad, M., & Sama, F. (2019). Topology, magnetism and dye adsorption properties of metal organic frameworks (MOFs) synthesized from bench chemicals. *CrystEngComm*, 21(35), 5299–5309. <https://doi.org/10.1039/C9CE01041F>
- Kamal, S., Khalid, M., Khan, M. S., Shahid, M., Ashafaq, M., Mantasha, I., Ahmad, M. S., Ahmad, M., Faizan, M., & Ahmad Inorg, S. (2020). *Chimica Acta*, 512, 119872.

- Karlin, K. D., Nasir, M. S., Cohen, B. I., Cruse, R. W., Kaderli, S., & Zuberbuehler, A. D. (1994). Reversible dioxygen binding and aromatic hydroxylation in O₂-reactions with substituted Xylyl dinuclear copper(I) complexes: Syntheses and low-temperature kinetic/thermodynamic and spectroscopic investigations of a copper monooxygenase model system. *Journal of the American Chemical Society*, 116(4), 1324–1336. <https://doi.org/10.1021/ja00083a018>
- Karlin, K. D., Wei, N., Jung, B., Kaderli, S., Niklaus, P., & Zuberbuehler, A. D. (1993). Kinetics and thermodynamics of formation of copper-dioxygen adducts: oxygenation of mononuclear copper(I) complexes containing tripodal tetradentate ligands. *Journal of the American Chemical Society*, 9506–9514. <https://doi.org/10.1021/ja00074a015>
- Khan, M. S., Hayat, M. U., Khanam, M., Saeed, H., Owais, M., Khalid, M., Shahid, M., & Ahmad, M. (2020). *Journal of Biomolecular Structure and Dynamics*, <https://doi.org/10.1080/07391102.2020.1776156>.
- Khan, M. S., Khalid, M., Ahmad, M. S., & Shahid, M., & Ahmad, M. (2020). Catalytic activity of Mn(III) and Co(III) complexes: evaluation of catechol oxidase enzymatic and photodegradation properties. *Research on Chemical Intermediates*, 46, 2985–3006.
- Khan, M. S., Khalid, M., Ahmad, M. S., Shahid, M., & Ahmad, M. (2019). Design and Characterization of a Cu(II) Coordination Polymer Based on α -Diimine: Evaluation of the Biomimetic Activity. *Journal of Structural Chemistry*, 60(11), 1833–1841. <https://doi.org/10.1134/S0022476619110180>
- Khan, M. S., Khalid, M., Ahmad, M. S., Shahid, M., & Ahmad, M. (2019). Three-in-one is really better: Exploring the sensing and adsorption properties in a newly designed metal-organic system incorporating a copper(II) ion. *Dalton Transactions (Cambridge, England : 2003)*, 48(34), 12918–12932. <https://doi.org/10.1039/c9dt02578b>
- Khan, M. S., Khalid, M., & Shahid, M. (2021). A Co(II) coordination polymer derived from pentaerythritol as an efficient photocatalyst for the degradation of organic dyes. *Polyhedron*, 196, 114984. <https://doi.org/10.1016/j.poly.2020.114984>
- Khan, M. S., Khalid, M., & Shahid, M. (2021). Engineered Fe 3 triangle for the rapid and selective removal of aromatic cationic pollutants: Complexity is not a necessity. *RSC Advances*, 11(5), 2630–2642. <https://doi.org/10.1039/D0RA09586A>
- Khan, M. S., Khalid, M., & Shahid, M. (2020). What triggers dye adsorption by metal organic frameworks? The current perspectives. *Materials Advances*, 1(6), 1575–1601. <https://doi.org/10.1039/D0MA00291G>
- Khan, M. S., Khalid, M., Ahmad, M. S., Ahmad, M., Ashafaq, M., Rahisuddin, Arif, R., & Shahid, M. (2019). Synthesis, spectral and crystallographic study, DNA binding and molecular docking studies of homo dinuclear Co(II) and Ni(II) complexes. *Journal of Molecular Structure*, 1175, 889–899. <https://doi.org/10.1016/j.molstruc.2018.08.048>
- Kitos, A. A., Efthymiou, C. G., Papatriantafyllopoulou, C., Nastopoulos, V., Tasiopoulos, A. J., Manos, M. J., Wernsdorfer, W., Christou, G., & Perlepes, S. P. (2011). The search for cobalt single-molecule magnets: A disk-like Co(II) cluster with a ligand derived from a novel transformation of 2-acetylpyridine. *Polyhedron*, 30(18), 2987–2996. <https://doi.org/10.1016/j.poly.2011.02.013>
- Koval, I. A., Gamez, P., Belle, C., Selmecci, K., & Reedijk, J. (2006). Synthetic models of the active site of catechol oxidase: mechanistic studies. *Chemical Society Reviews*, 35(9), 814–840. <https://doi.org/10.1039/b516250p>
- Koval, I. A., Selmecci, K., Belle, C., Philouze, C., Saint-Aman, E., Gautier-Luneau, I., Schuitema, A. M., Vliet, M. v., Gamez, P., Roubeau, O., Lütken, M., Krebs, B., Lutz, M., Spek, A. L., Pierre, J.-L., & Reedijk, J. (2006). Catecholase activity of a copper(II) complex with a macrocyclic ligand: Unraveling catalytic mechanisms. *Chemistry (Weinheim an Der Bergstrasse, Germany)*, 12(23), 6138–6150. <https://doi.org/10.1002/chem.200501600>
- Krause, R. A., Colthup, N. B., & Busch, D. H. (1961). Infrared spectra of complexes of 2-pyridinaldoxime. *The Journal of Physical Chemistry*, 65(12), 2216–2219. <https://doi.org/10.1021/j100829a026>
- Lawrence, J., Beedle, C. C., Yang, E.-C., Ma, J., Hill, S., & Hendrickson, D. N. (2007). High frequency electron paramagnetic resonance (HFEP) study of a high spin Co(II) complex. *Polyhedron*, 26(9–11), 2299–2303. <https://doi.org/10.1016/j.poly.2006.11.018>
- Lever, A. B. P. (1984). *Inorganic electronic spectroscopy*. Elsevier.
- Liu, Y., Wu, H., Chong, Y., Wamer, W. G., Xia, Q., Cai, L., Nie, Z., Fu, P. P., & Yin, J. J. (2015). Platinum nanoparticles: Efficient and stable catechol oxidase mimetics. *ACS Applied Materials & Interfaces*, 7(35), 19709–19717. <https://doi.org/10.1021/acsami.5b05180>
- Mariyam, A., Shahid, M., Mantasha, I., Khan, M. S., & Ahmad, M. S. (2020). Tetrazole based porous metal organic framework (MOF): Topological analysis and dye adsorption properties. *Journal of Inorganic and Organometallic Polymers and Materials*, 30(6), 1935–1943. <https://doi.org/10.1007/s10904-019-01334-6>
- Mergehenn, R., & Haase, W. (1977). The crystal structure of cyanato(2-dimethylaminoethanolato)copper(II), C₅H₁₀ N₂ O₂Cu. *Acta Crystallographica Section B: Structural Crystallography and Crystal Chemistry*, 33(6), 1877–1882. <https://doi.org/10.1107/S0567740877007249>
- Merz, L., & Haase, W. (1978). Crystal and molecular structure and magnetic properties of tetrakis-[(2-diethylaminoethanolato)isocyanato]copper(II). *Journal of the Chemical Society, Dalton Transactions*, (11), 1594–1598. <https://doi.org/10.1039/dt9780001594>
- Merz, L., & Haase, W. (1980). Exchange interaction in tetrameric oxygen-bridged copper(II) clusters of the cubane type. *Journal of the Chemical Society, Dalton Transactions*, (6), 875–879. <https://doi.org/10.1039/dt9800000875>
- Mijangos, E., Reedijk, J., & Gasque, L. (2008). Copper(II) complexes of a polydentate imidazole-based ligand. pH effect on magnetic coupling and catecholase activity. *Dalton Transactions*, (14), 1857. <https://doi.org/10.1039/b714283h>
- Mueller-Westerhoff, U. T., Nazzari, A., & Proessdorf, W. (1981). First evidence for the existence of intramolecular carbon-hydrogen-carbon hydrogen bonds: carbanions of [1.1]ferrocenophane, 1-methyl-[1.1]ferrocenophane, and 1,12-dimethyl-[1.1]ferrocenophane. *Journal of the American Chemical Society*, 103(25), 7678–7681. <https://doi.org/10.1021/ja00415a059>
- Nakamoto, K. (1986). *Infrared and Raman Spectra of inorganic and coordination compounds*. Wiley.
- Ording-Wenker, E. C. M., Siegler, M. A., Lutz, M., & Bouwman, E. (2015). Catalytic catechol oxidation by copper complexes: Development of a structure–activity relationship. *Dalton Transactions (Cambridge, England: 2003)*, 44(27), 12196–12209. <https://doi.org/10.1039/c5dt01041a>
- Papadakis, R., Rivière, E., Giorgi, M., Jamet, H., Rousselot-Pailley, P., Réglie, M., Simaan, A. J., & Tron, T. (2013). Structural and magnetic characterization of a tetranuclear copper(II) cubane stabilized by intramolecular metal cation- π interactions. *Inorganic Chemistry*, 52(10), 5824–5830. <https://doi.org/10.1021/ic3027545>
- Punniyamurthy, T., Velusamy, S., & Iqbal, J. (2005). Recent advances in transition metal catalyzed oxidation of organic substrates with molecular oxygen. *Chemical Reviews*, 105(6), 2329–2364. <https://doi.org/10.1021/cr050523v>
- Que, L., & Tolman, W. B. (2008). Biologically inspired oxidation catalysis. *Nature*, 455(7211), 333–340.
- Sama, F., Ansari, I. A., Raizada, M., Ahmad, M., Nagaraja, C. M., Shahid, M., Kumar, A., Khan, K., & Siddiqi, Z. A. (2017). Design, structures and study of non-covalent interactions of mono-, di-, and tetranuclear complexes of a bifurcated quadridentate tripod ligand, N-(amino-propyl)-diethanolamine. *New Journal of Chemistry*, 41(5), 1959–1972. <https://doi.org/10.1039/C6NJ02562E>
- Sama, F., Dhara, A. K., Akhtar, M. N., Chen, Y.-C., Tong, M.-L., Ansari, I. A., Raizada, M., Ahmad, M., Shahid, M., & Siddiqi, Z. A. (2017). Aminoalcohols and benzoates-friends or foes? Tuning nuclearity of Cu(II) complexes, studies of their structures, magnetism, and catecholase-like activities as well as performing DFT and TDDFT studies. *Dalton Transactions (Cambridge, England : 2003)*, 46(30), 9801–9823. <https://doi.org/10.1039/c7dt01571b>
- Sénéque, O., Campion, M., Douzich, B., Giorgi, M., Rivière, E., Journaux, Y., Mest, Y. L., & Reinaud, O. (2002). Supramolecular Assembly with Calix[6]arene and copper ions – formation of a novel tetranuclear core exhibiting unusual redox properties and catecholase activity. *European Journal of Inorganic Chemistry*, 2002(8), 2007–2014. [https://doi.org/10.1002/1099-0682\(200208\)2002:8<2007::AID-EJIC2007>3.0.CO;2-Z](https://doi.org/10.1002/1099-0682(200208)2002:8<2007::AID-EJIC2007>3.0.CO;2-Z)
- Sessoli, R., Gatteschi, D., Caneschi, A., & Novak, M. A. (1993). Magnetic bistability in a metal-ion cluster. *Nature*, 365(6442), 141–143. <https://doi.org/10.1038/365141a0>

- Sessoli, R., Tsai, H.-L., Schake, A. R., Wang, S., Vincent, J. B., Folting, K., Gatteschi, D., Christou, G., & Hendrickson, D. N. (1993). High-spin molecules: $[\text{Mn}_{12}\text{O}_{12}(\text{O}_2\text{CR})_{16}(\text{H}_2\text{O})_4]$. *Journal of the American Chemical Society*, 115(5), 1804–1816. 1. <https://doi.org/10.1021/ja00058a027>
- Sheldrick, G. M. (2002). SADAS [software for empirical absorption correction, Ver. 2.05]. University of Göttingen.
- Sreenivasulu, B., Zhao, F., Gao, S., & Vittal, J. J. (2006). Synthesis, structures and catecholase activity of a new series of Dicopper(II) Complexes of reduced schiff base ligands. *European Journal of Inorganic Chemistry*, 2006(13), 2656–2670. <https://doi.org/10.1002/ejic.200600022>
- Tan, X. S., Fujii, Y., Nukada, R., Mikuriya, M., & Nakano, Y. (1999). Crystal structure and ferromagnetic behaviour of a novel tetranuclear copper(II) complex with an open cubane-like Cu_4O_4 framework. *Journal of the Chemical Society, Dalton Transactions*, (15), 2415–2416. <https://doi.org/10.1039/a903524i>
- Walz, L. H., Paulus, W., & Haase, J. (1983). *Chemistry Society, Dalton Transactions*, 6.
- Wegner, R., Gottschaldt, M., Görls, H., Jäger, E., & Klemm, D. (2001). Copper(II) complexes of aminocarbohydrate β -ketoenaminic ligands: efficient catalysts in catechol oxidation. *Chemistry*, 7(10), 2143–2157. [https://doi.org/10.1002/1521-3765\(20010518\)7:10<2143::AID-CHEM2143>3.0.CO;2-D](https://doi.org/10.1002/1521-3765(20010518)7:10<2143::AID-CHEM2143>3.0.CO;2-D)
- XPREP. (1995), version 5.1. Siemens Industrial Automation Inc.
- Yang, L., Powell, D. R., & Houser, R. P. (2007). Structural variation in copper(II) complexes with pyridylmethylamide ligands: Structural analysis with a new four-coordinate geometry index, τ_4 . *Dalton Transactions*, (9), 955–964. <https://doi.org/10.1039/B617136B>
- Yang, E.-C., Wernsdorfer, W., Zakharov, L. N., Karaki, Y., Yamaguchi, A., Isidro, R. M., Lu, G.-D., Wilson, S. A., Rheingold, A. L., Ishimoto, H., & Hendrickson, D. N. (2006). Fast magnetization tunneling in Tetranickel(II) single-molecule magnets. *Inorganic Chemistry*, 45(2), 529–546. <https://doi.org/10.1021/ic050093r>
- Zhang, X.-Y., Li, B., Tang, J.-K., Tian, J.-M., Huang, J.-L., & Zhang, J.-P. (2013). Tuning the interactions from antiferro- to ferro-magnetic by molecular tailoring and manipulating. *Dalton Transactions (Cambridge, England: 2003)*, 42(10), 3308–3317. <https://doi.org/10.1039/c2dt32021e>